Ab Initio Simulation of Carbon Clustering on an Ni(111) Surface: A Model of the Poisoning of Nickel-Based Catalysts†

G. Kalibaeva

Dipartimento di Fisica, Università degli Studi di Roma "La Sapienza", Piazzale Aldo Moro 6, 00185, Roma, Italy

R. Vuilleumier

Laboratoire de Physique Thèorique de la Matière Condensée, Université Pierre et Marie Curie, 4 place Jussieu, F-75005 Paris, France

S. Meloni*

CASPUR − Consorzio per le Appicazione del Supercalcolo, per Università e Ricerca, via dei Tizii, 6b, 00185, Roma, Italy

A. Alavi

Department of Chemistry, University of Cambridge, Lensfield Road, Cambridge CB2 1TQ, U.K.

G. Ciccotti

INFM and Dipartimento di Fisica, Università degli Studi di Roma "La Sapienza", Piazzale Aldo Moro 6, 00185, Roma, Italy

R. Rosei

INFM and Dipartimento di Fisica, Università degli Studi di Trieste, via Valerio 2, 34012, Trieste, Italy

Received: September 22, 2005; In Final Form: December 7, 2005

In this work, we studied the poisoning of a nickel surface due to carbon. Performing ab initio simulations, within the framework of density functional theory, we computed the surface energy of the nickel (111) surface as a function of carbon coverage. On the basis of these results, we can assert that the stable state of the nickel/carbon surface is either a clean nickel surface or a fully carbon-covered nickel surface, which has a graphitic configuration. The relative stability of the two states depends on the temperature and partial pressure of the carbon gas. At fixed nominal carbon coverage, the most stable configurations are those forming carbon clusters. However, the nickel sites hosting these clusters change from hexagonal close packed/face centered cubic (hcp/fcc) sites to on-top sites when going toward larger clusters. This indicates that poisoning due to graphitic patches occurs on on-top sites.

1. Introduction

Transition metal catalysts are used in a large number of industrially important reactions, such as methanation. In this reaction, methane is synthesized from steam reforming products, CO and H_2. One of the most active methanation catalysts, nickel, is able to dissociate CO and subsequently form methane.[1,2] Some computer simulation studies of the methanation process have already been carried out.[3] In the initial step of this process, carbon absorption on the nickel surface occurs. There are two main carbon phases identified. The first one is the active carbon phase leading to hydrocarbon product formation, named the "carbidic" phase. In this phase, reactive carbon atoms are distributed more or less uniformly over the surface. This implies that in this phase, which we will call hereafter "disperse", the coverage cannot be too high since a high packing will induce clustering and therefore reduce reactivity. The second phase is the inactive carbon phase leading to catalyst deactivation, named the "graphitic" phase. In this phase, a graphite monolayer bonded to the surface is formed and the catalyst is rendered inactive.

In general, the poisoning of a catalyst can be "temporary", which means that the catalyst can be recovered performing some treatment, or "permanent", if the catalyst cannot be restored. The graphitic carbon layer on a transition metal surface produces permanent poisoning.

Our goal is to study, from first principles, the poisoning of the nickel (111) surface due to the formation of carbon clusters. We want to investigate whether carbon atoms assume a dispersed configuration or prefer to cluster. In the latter case, we also want to investigate their configuration. It is worth mentioning perhaps at this point that the Ni(111) surface is a particularly favorable surface to create a graphene overlayer since there is a good geometrical matching between the lattice parameters of Ni(111) and the graphene monolayer.

† Part of the special issue "Michael L. Klein Festschrift".

* To whom correspondence should be addressed. E-mail: simone.meloni@caspur.it.

10.1021/jp055397d CCC: $33.50
Published on Web 01/17/2006

In our calculations, we used the CPMD (Car−Parrinello molecular dynamics) program,[4] with the free energy functional approximation, proposed by Alavi, Kohanoff, Parrinello, and Frenkel in 1994.[5]

In the following section, we describe the theory of absorption of carbon atoms and formation of the cluster on the nickel surface, in the third and forth sections, we describe our system and present the computational setup and results, in the fifth section, we perform finite temperature and pressure analyses, and in the last section, we draw some conclusions.

2. Theory of Absorption on Surfaces

The stability of surfaces is governed by surface free energy σ

$$\sigma(T,P;x) = \frac{1}{A}(G_s - \sum_i \mu_i N_i) \quad (1)$$

where G_s is the Gibbs energy of the surface, μ_i is the chemical potential of the pure chemical species i in its reference state at the same pressure P and temperature T, N_i is the number of atoms of species i, A is the surface area, and x is the carbon coverage. $x = 1$ refers to "full-coverage", which in the present system we define to be two carbon atoms per surface unit cell, which corresponds to a monolayer of graphite absorbed on the surface, and $x = 0$ refers to the clean surface, the one with no carbon atoms absorbed. The sum runs over the chemical species, carbon and nickel in our case. At equilibrium, at a given temperature and pressure, the coverage x is the one which minimizes the surface free energy.

We can rewrite eq 1 as a function of temperature T explicitly. For that, we have to substitute in eq 1 the expression for the Gibbs free energy G_s. In this paper, we discard the effect of pressure on solid phases, therefore we assume that the value of the enthalpy H is equivalent to the value of internal energy E, so that

$$G_s = E - TS = E - TS_{thermal} - Tk_B \ln W_S \quad (2)$$

where $S_{thermal}$ is the thermal entropy of the surface and the last term is the configurational entropy. In the last term, k_B is the Boltzmann constant and W_S is the number of equivalent configurations of carbon atoms on the Ni surface at a given coverage x. The chemical potential μ_{Ni} for nickel is

$$\mu_{Ni} = \frac{G_{Ni}}{N_{Ni}} = \frac{E^{Ni}(T) - TS_{Ni}(T)}{N_{Ni}} \quad (3)$$

with E^{Ni} the internal energy and $S_{Ni}(T)$ the enthropy of the face centered cubic (fcc) nickel perfect crystal at temperature T. The reference state we use for carbon is gas, which we approximate as an ideal gas

$$\mu_C(T,P_C) = \mu_C(T,P^*) + k_B T \log[P_C/P^*] \quad (4)$$

where P_C is the actual carbon partial pressure and P^* is a reference pressure for which the chemical potential of carbon is known. Denoting the enthropy per atom in the bulk nickel phase S_{Ni}/N_{Ni} as s_{Ni} and the energy per atom, E^{Ni}/N_{Ni} as e^{Ni}, we get the surface energy dependence on temperature

$$\sigma(T,P_C;x) = \frac{1}{A}[E - TS_{thermal} - Tk_B \ln W_S - N_C\mu_C(T,P_C) - N_{Ni}(e^{Ni}(T) - Ts_{Ni}(T))] \quad (5)$$

Equation 5 requires the chemical potential of carbon gas. This chemical potential can be obtained by writing the equilibrium condition between the carbon vapor and the graphite, that is, at saturation pressure, P_{sat}

$$\mu_C(T,P_{sat}(T)) = \mu_{graph}(T,P_{sat}(T)) \quad (6)$$

neglecting the variations of the graphite chemical potential with pressure

$$\mu_{graph}(T,P) = \mu_{graph}(T,P_{sat}(T)) \quad (7)$$

and substituting eq 4 into eq 6, we obtain

$$\mu_C(T,P) + k_B T \log[P_{sat}(T)/P] = \mu_{graph}(T,P) \quad (8)$$

Therefore, we can write

$$\mu_C(T,P) = \mu_{graph}(T,P) + k_B T \log[P/P_{sat}(T)] \quad (9)$$

As we have done for bulk nickel, we rewrite the chemical potential of graphite as (ignoring pressure effects)

$$\mu_{graph}(T) = \frac{G_{graph}}{N_{graph}} = \frac{E^{graph}(T) - TS_{graph}(T)}{N_{graph}} \quad (10)$$

Therefore, we can rewrite eq 5 as

$$\sigma(T,P_C;x) = \sigma^0(T,P_{sat};x) - \frac{N_C}{A} k_B T \log[P_C/P_{sat}(T)] \quad (11)$$

with

$$\sigma^0(T,P_{sat};x) = \frac{1}{A}[E - TS_{thermal} - k_B T \ln W_S - N_C(e^{graph}(T) - Ts_{graph}(T)) - N_{Ni}(e^{Ni}(T) - Ts_{Ni}(T))] \quad (12)$$

where we denote the enthropy per atom for graphite S_{graph}/N_{graph} as s_{graph} and the energy per atom E^{graph}/N_{graph} as e^{graph}. In the following, we assume that we can neglect the vibrational contributions to the difference between the thermal entropy of our system composed of the nickel surface and carbon adatoms and the bulk nickel plus graphite thermal entropies. A calculation of these terms, in the harmonic approximation, from an analysis of the normal modes would be prohibitively expensive while an estimate of the order of magnitude of the vibrational contribution to the pure Ni surface energy from the Debye approximation (see ref 6), applicable to that case and using data from ref 7, showed that it should not alter the quality of our results. From the previous equation, we now define a reference surface energy as the zero temperature limit of σ^0

$$\sigma^r(x) = \frac{1}{A}[E - N_C \times e^C - N_{Ni} \times e^{Ni}] \quad (13)$$

We then get a final expression for the surface energy as a function of temperature, pressure, and coverage

$$\sigma(T,P_C;x) = \sigma^r(x) - \frac{1}{A} k_B T \ln W_S - \frac{N_C}{A} k_B T \log[P_C/P_{sat}(T)] \quad (14)$$

The equilibrium coverage depends on the shape of $\sigma(T,P_C;x)$ with respect to coverage x. This behavior can be better understood referring to an ideal two-step mechanism. In the first step, a carbon layer with a given coverage superposed to a nickel surface is formed. If the curve is convex (Figure 1, right panel),

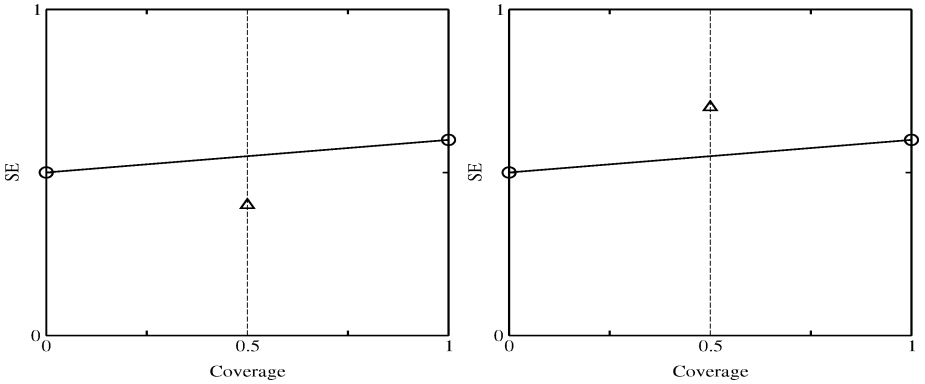

Figure 1. On the left, the surface energy of an intermediate state (triangle) is lower than that of the linear combination of the two reference states with $x = 0$ and $x = 1$ (circles): the intermediate state is more stable (we obtain a concave curve). On the right, the surface energy of the intermediate state (triangle) is higher than that of the linear combination of the two reference states (circles): the system will split into two zones, one with $x = 0$, the other with $x = 1$ (we obtain a convex curve).

the surface energy would be minimal if the system splits into two phases, one at $x = 1$ and another at $x = 0$. That is, the linear combination of surface energy of the clean and fully covered surface

$$\sigma_{lc}(x) = x\sigma_{(x=1)} + (x - 1)\sigma_{(x=0)} \tag{15}$$

is lower than the surface energy of the system at the uniform coverage x. Therefore, if we neglect the line tension between the two phases, $x = 1$ and $x = 0$, the stable state is a coexistence of the two phases with the amounts of phases given by the lever rule. On the other hand, if the curve is concave (Figure 1, left panel), then the surface energy of the system in this state is the minimum achievable for this given nominal composition and the system is stable. That is, the surface energy of the linear combination of the pure phases, eq 15, is higher than the surface energy of the system uniformly covered, which remains in this state. In the second step, the surface generated during the first step is put in contact with the carbon gas phase. The complete system will equilibrate bringing the surface energy to a minimum with respect to the coverage x.

$$\sigma(T,P_C;x_{obs}) = \min_x \sigma(T,P_C;x) \tag{16}$$

In the second step, there are two cases as well. In the first case, if the curve is concave, then the equilibrium coverage will be the one corresponding to the minimum of the surface energy, which occurs at coverage x_{obs}. Therefore, depending on the fact that the nominal composition x is lower or higher than x_{obs} carbon will be absorbed onto or desorbed from the nickel surface. If the curve is convex, then the equilibrium surface will be either the fully covered or the clean one, depending on their relative surface energies.

The surface energy, eq 1, can be understood as a function of composition and configuration. Both composition and configuration are then internal variables of the system with respect to which the surface energy at equilibrium should be minimized. It is natural to first minimize with respect to all possible uniform, not necessarily ordered, configurations at fixed composition and then treat the latter as an internal variable. The observed coverage, x_{obs}, the one which minimizes the surface energy, eq 16, is itself a function of temperature and partial pressure of carbon. However, in practice, we cannot span all the configurational space corresponding to given coverages. The number of configurations allowed is mainly limited by our system size and the use of periodic boundary conditions (PBCs). To be as exhaustive as possible in performing this search, we performed geometry optimizations with a few different starting configurations. When this resulted to more than one final configuration, only the one with the lowest surface energy was retained to determined the surface energy corresponding to that composition. This practical scheme was already used in previous papers giving good results.[8]

In the following, we will calculate the surface free energy of a nickel slab including an increasing number of carbon atoms. At each coverage, we will find, by geometry optimization, the lowest energy configuration. We will then plot the surface free energy as a function of coverage and conclude about the clustering properties of carbon on nickel depending on the convex or concave shape of that curve.

3. Computational Details

We simulate a periodic system, consisting of a nickel (111) surface with carbon atoms absorbed on it at different configurations. No carbon atoms in vapor phase were included in our simulations.

We performed geometry optimization of the different systems corresponding to a clean and covered surface at various concentrations and configurations. All calculations were carried out using the CPMD program.[4] We have employed free energy density functional theory (AKPF)[5] with a 3×3 k-points sampling in the same plane as the surface and an electronic temperature of 1000 K. Wave functions were expanded on a basis set of plane waves with a kinetic energy cutoff of $E_c = 70$ Ry.

All calculations were performed imposing zero magnetization. It was already shown that while the effect on binding energies is important this approximation introduces negligible errors on the difference of binding energies among different binding sites and for different coverages,[9,10] which is the topic of the present study.

We have generated a Troullier−Martins[11] norm conserving pseudopotential for Ni using the Atom package written by Giannozzi and collaborators, with the Perdew−Burke−Ernzerhof (PBE)[12] functional. The 3d, 4s, and 4p electrons of nickel were treated as valence electrons with a pseudization radius r_c equal to 2.05 au, 2.24 au, and 3.14 au, respectively. The lattice parameter obtained for the Ni fcc bulk metal crystal was 6.769 au, which is near to the experimental value of 6.659 au.

Also for carbon, we generated a Trouiller−Martins norm conserving pseudopotential with the PBE functional. The 1s state was treated as a core state, and the 2s and 2p were treated as valence states. The pseudization radius for both valence states

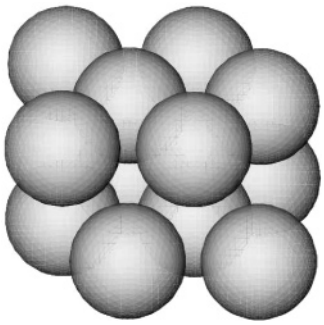

Figure 2. Simulation cell: top view of the Ni(111) surface.

was taken as 1.23 au. The lattice parameter obtained for diamond bulk using this potential is 6.758 au, close to the experimental value of 6.743 au.

We have taken as reference states for the calculation of the chemical potential of nickel the fcc crystal and for carbon the graphite structure. Nickel crystal was simulated using a supercell containing 12 Ni atoms arranged in three layers, four atoms in each layer; for graphite, the supercell contains eight carbon atoms in one layer. The boundary conditions were taken as periodic.

The nickel surface was represented by a periodic three-layer slab (four nickel atoms per layer, bottom layer fixed to the crystal geometry) followed by nine layers of vacuum. The initial interlayer distance was 3.9081 au. The top view of the simulation cell is presented in Figure 2.

Using eq 13, we have obtained the reference surface energy of the clean Ni(111) surface at zero temperature and pressure. This value corresponds to the zero carbon coverage, one of the main reference states of the system. The value obtained for the reference surface energy is

$$\sigma^r = 2.01 \text{ J/m}^2$$

in good agreement with the value of 2.02 J/m^2, reported in ref 13, and with the experimental value of 2.38 J/m^2, reported in ref 14, and 2.45 J/m^2, reported in ref 15.

The initial carbon configurations on the Ni surface were formed placing carbon atoms on the three stable positions, mentioned in eqs 13 and 16, which are the on-top, hexagonal close packed (hcp), and fcc sites, at the same distance from the nickel surface as the nickel interlayer separation. The on-top sites are situated over the atoms of the surface last layer, the hcp sites over those of the intermediate layer, and the fcc sites over those of the bottom layer.

4. Results

4.1. Absorption of One Atom on the Ni Surface. We performed geometry optimization placing one atom on the on-top, hcp, and fcc sites over the Ni surface, at the same distance as the interlayer distance between the Ni layers in the slab. The reference surface energies obtained, eq 13, are

$$\text{C atom in the on-top site: } \sigma^r = 3.24 \text{ J/m}^2$$

$$\text{C atom in the hcp site: } \sigma^r = 2.40 \text{ J/m}^2$$

$$\text{C atom in the fcc site: } \sigma^r = 2.41 \text{ J/m}^2$$

As in eq 13, the lowest surface energy corresponds to the hcp site, followed by the fcc site. The position less convenient energetically is the on-top site.

After geometry optimization, the distances between the carbon atom and the nickel surface are

$$\text{C atom in the on-top site: } d = 2.98 \text{ au}$$

$$\text{C atom in the hcp site: } d = 1.91 \text{ au}$$

$$\text{C atom in the fcc site: } d = 1.95 \text{ au}$$

Here and in the following we define the distance between the carbon atom(s) and the nickel surface as the difference between the vertical coordinate of the carbon atom(s) and the average of the vertical coordinates of the nickel atoms forming the surface layer.

4.2. Complete Coverage: Graphite Monolayer. To simulate the complete coverage, we have produced three initial configurations: the first one placing the carbon atoms in all the on-top and hcp sites, the second in all the on-top and fcc sites, and the third in all the hcp and fcc sites.

When carbon atoms forming the graphite monolayer (GM) are placed on fcc and hcp sites, as suggested in refs 17 and 18, they are drawn away during the geometry optimization, that is, no stable configuration was found in this case. When van der Waals terms are included, such a configuration could exist but, then, it would barely be stable. Instead, the other two initial configurations we used are stable and have surface energies

$$\text{GM in the on-top and hcp sites: } \sigma^r = 1.89 \text{ J/m}^2$$

$$\text{GM in the on-top and fcc sites: } \sigma^r = 1.85 \text{ J/m}^2$$

On the basis of these data, we can say that the most stable positions for the atoms in the graphitic monolayer are the on-top and fcc sites, which coincide with the previous experimental data.[19−22] The top views of the final configurations are presented in Figure 3.

The vertical distances between the carbon atoms and the Ni surface are

GM in the on-top and hcp sites

$$\text{on-top sites: } d = 4.03 \text{ au}$$

$$\text{hcp sites: } d = 4.04 \text{ au}$$

GM in the on-top and fcc sites

$$\text{on-top sites: } d = 4.02 \text{ au}$$

$$\text{fcc sites: } d = 4.03 \text{ au}$$

The values of the distances are very similar among them and close to the interlayer distance of the Ni slab.

4.3. Disperse Carbon Atoms on the Ni Surface. We generated "disperse" carbon configurations up to 1/2 coverage. We consider disperse those configurations in which carbon−carbon distances are larger than the typical carbon−carbon bond length. Here, we consider bonded two carbon atoms if their distance is lower than 3 au.

Among all the possible disperse configurations, we consider only those in which atoms are placed on sites of the same kind, hcp or fcc, that is, the sites more convenient energetically (see section 4.1). Starting from the initial configurations defined above, we performed geometry optimization. We limited our simulation to 1/4 and 1/2 coverages, for which there is only one independent configuration. Four simulations have been carried out: two carbon atoms (1/4 of coverage) either in hcp or in fcc sites and four carbon atoms (1/2 of coverage) either in

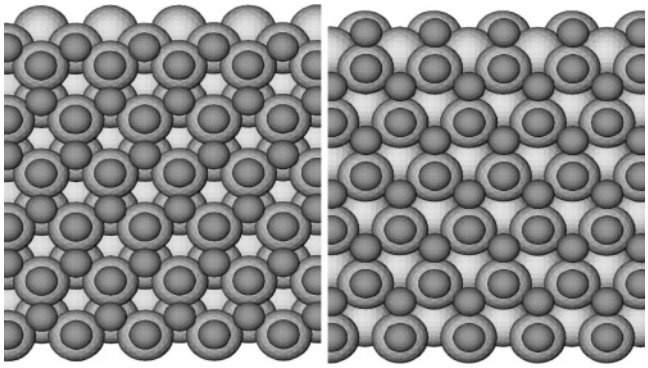

Figure 3. Top view of geometry-optimized configurations of the graphite monolayer on the Ni surface initially in on-top and hcp (left) and on-top and fcc (right) positions. Big circles represent Ni atoms, and small, darker circles represent C atoms.

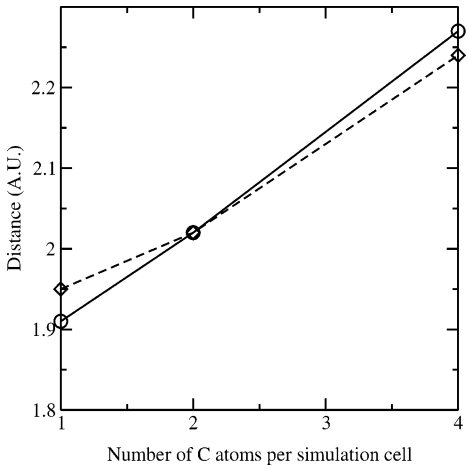

Figure 4. Distance between the dispersed carbon atoms in hcp (circles) and fcc (diamonds) sites as a function of carbon coverage. Four atoms of carbon per simulation cell correspond to half-coverage.

hcp or in fcc sites. The resulting vertical distances between the carbon atoms and the Ni surface in each case are

two atoms in the hcp sites: $d = 2.02$ au

two atoms in the fcc sites: $d = 2.02$ au

4 atoms in the hcp sites: $d = 2.27$ au

four atoms in the fcc sites: $d = 2.24$ au

As we can observe, the equilibrium distance between the carbon and the surface is significantly less than the interlayer slab distance, and it increases with the carbon concentration on the surface. Figure 4 represents the distance between the carbon atoms and the nickel surface for disperse carbon configurations as a function of coverage.

The reference surface energies obtained, eq 13, are

two atoms in the hcp sites: $\sigma^r = 3.33$ J/m^2

two atoms in the fcc sites: $\sigma^r = 3.32$ J/m^2

four atoms in the hcp sites: $\sigma^r = 6.33$ J/m^2

four atoms in the fcc sites: $\sigma^r = 6.30$ J/m^2

Figure 5 displays the reference surface energies of disperse carbon configurations at different coverages.

We can see that all the surface energies at intermediate coverage configurations are greater than the linear combination of the empty surface and the full coverage ones. The dependence on carbon coverage of the surface energy calculated in the present work have a trend similar to the one of the binding energy reported in ref 16.

4.4. Carbon Forming Compounds on the Ni Surface: Geometry. We have simulated different carbon periodic patches, corresponding to different coverages, to see the influence of possible C−C bonds (applying the same definition of bonded carbon atoms given in section 4.3) on the surface energy at a given coverage. In each case, we have performed geometry optimization of initial configurations and calculated the reference surface energy.

We started with a pair of carbon atoms (corresponding to coverage 1/4) in three initial configurations, placing atoms on the on-top and hcp, on-top and fcc, and fcc and hcp sites, followed by geometry optimization of the system. Interestingly, all three cases relaxed to almost the fcc and hcp configurations. For the final configuration, the distance between the carbon atoms and the nickel surface is

$$d = 2.36 \text{ au}$$

The side view of this configuration is presented in Figure 10.

Increasing the coverage to 3/8, we have simulated three-atom carbon compounds (trimers) on the nickel surface. All the three-atom initial configurations relax to two different final configurations: in one of them, the two side atoms are placed on the hcp sites and the central one is in the bridge position between the fcc and on-top sites; in the other, the two side atoms are placed in the fcc sites and the central one is in the bridge position between the on-top and hcp sites. The distances between the carbon atoms and the nickel surface are

hcp−bridge−hcp

hcp sites (side atoms): $d = 2.38$ au

bridge site (central atom): $d = 3.54$ au

fcc−bridge−fcc

fcc sites (side atoms): $d = 2.36$ au

bridge site (central atom): $d = 3.50$ au

The distances between the middle atom and the surface are higher than the distances between the side atoms and the surface. The two final configurations for the three-atom compounds are presented in Figure 6. The side view of the fcc−bridge−fcc configuration is presented in Figure 10.

In the case of half-coverage (four carbon atoms per simulation cell), we have initially positioned carbon atoms forming trans and cis infinite chains. There are three possible placement for the two kind of chains, carbon atoms can be alternated on the hcp and fcc sites, hcp and on-top sites, and fcc and on-top sites. One trans and cis initial configurations are presented in Figure 7.

After geometry optimization, the cis four-atom relaxed configurations have significantly higher surface energy than the trans ones (about 15% more) and, therefore, are less stable. So we will focus only on the trans configurations, presented in Figure 8.

As we can observe, the three trans infinite chains relax to structures very similar geometrically, even though the sites occupied by carbon atoms are different in the three cases. The

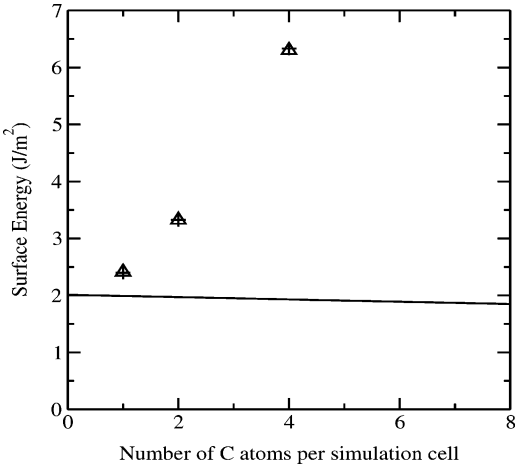

Figure 5. Surface energy as a function of the carbon coverage for disperse carbon atoms on the Ni(111) surface. The triangles (△) correspond to all carbon atoms on the hcp sites and the crosses (+) on the fcc sites. Eight carbon atoms correspond to full coverage. The line corresponds to the surface energy defined in eq 15.

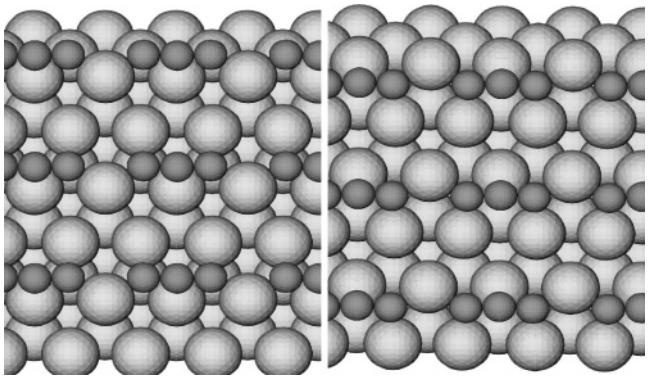

Figure 6. Two final configurations for carbon atoms forming trimers on the nickel surface, top view. The figure was obtained taking into account the periodic boundary conditions. Same representation as in Figure 3.

lowest energy configuration was obtained starting from the initial configuration (IC) which correspond to the trans chain placed on the fcc and on-top sites (see Figure 8). The side view of the final lowest energy configuration (fcc and bridge sites) is presented in Figure 10.

The distances between the carbon atoms and the nickel surface in the relaxed trans configurations are

IC in on-top and hcp sites

almost-hcp sites (two atoms): $d = 3.08$ au

bridge sites (two atoms): $d = 3.69$ au

IC in on-top and fcc sites

almost-fcc sites (two atoms): $d = 3.08$ au

bridge site (two atoms): $d = 3.70$ au

IC on hcp and fcc sites

almost-hcp sites: $d = 3.30$ au

almost-fcc sites: $d = 3.03$ au

For the 3/4 coverage, we put six carbon atoms per simulation cell, forming rings on the nickel surface. One of the initial configurations (with the carbon atoms in the fcc and hcp sites) remains almost the same after geometry optimization, while the other two (with carbon atoms initially in on-top and hcp for the first and on-top and fcc for the second configuration) relax to the same structure with all the carbon atoms in bridge positions (see Figure 9). The side view of this bridge structure is presented in Figure 10, where we can see that, when all the

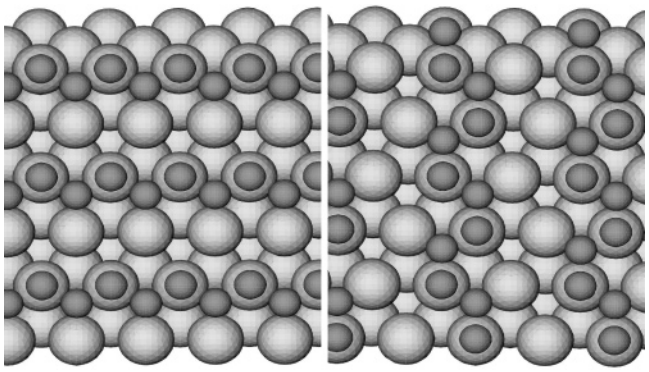

Figure 7. Two of the initial configurations for half-coverage, carbon forming infinite trans (left) and cis (right) chains on the nickel surface, top view.

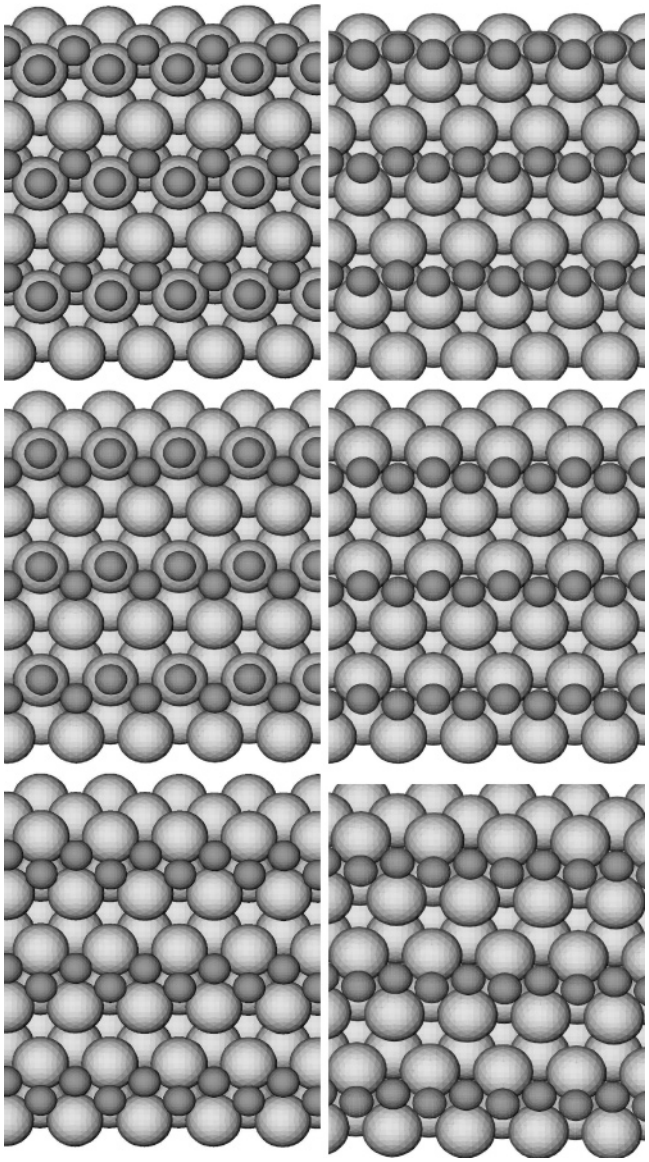

Figure 8. Carbon atoms forming infinite trans chains on the nickel surface. The initial configurations are on the left, and the final configurations are on the right, top view.

carbon atoms are in bridge positions, one of the nickel atoms goes up almost at the same distance of the carbon atoms from the surface. Here, when calculating the distance between the carbon atoms and the nickel surface, we are not taking into account the nickel atom which left the surface (see Figure 10). This can be explained by the fact that the infinite structure obtained represents a graphitic sheet with vacancies, filled by nickel atoms, which move up into the graphitic layer. Actually, these kinds of mixed C−Ni phases have already been observed in experiments.[23] It is interesting to remark that this structure has a much lower energy than the structure with all C atoms in fcc and hcp positions, in which the Ni atoms do not move up.

For these systems, the distances between the carbon atoms and the nickel surface for each configuration are

Bridge configuration:

side of the ring (four atoms): $d = 3.58$ au

middle atoms (two atoms): $d = 3.87$ au

hcp and fcc configuration:

side of the ring (four atoms): $d = 2.92$ au

middle atoms (two atoms): $d = 3.50$ au

To summarize this section, Figure 11 shows the dependence on the carbon coverage of the average distance between the lowest energy carbon compounds and the nickel surface. It can be seen that the carbon−nickel distance increases monotonically with coverage.

Finally, it is worth noticing that the six-atom compound is not planar while the four-atom compound is planar.

4.5. Carbon Forming Compounds on the Ni Surface: Energetics. The reference surface energies for the final configurations, obtained after geometry optimization, are

two atoms

Pair in the fcc and hcp sites: $\sigma^r = 2.66$ J/m^2

three atoms

hcp−bridge−hcp: $\sigma^r = 3.10$ J/m^2

fcc−bridge−fcc: $\sigma^r = 3.07$ J/m^2

four atoms, trans infinite chains

Bridge and almost-hcp sites: $\sigma^r = 3.08$ J/m^2

Bridge and almost-fcc sites: $\sigma^r = 3.06$ J/m^2

Almost-hcp and -fcc sites: $\sigma^r = 3.13$ J/m^2

six atoms, rings

Bridge configuration: $\sigma^r = 3.27$ J/m^2

fcc and hcp configuration: $\sigma^r = 4.10$ J/m^2

Comparing these results with those of section 4.3 (see Figure 5), we can observe, that the surface energy of the two- and four-atom compounds is much lower than the surface energy of disperse configurations at the same coverage, confirming the formation of the C−C bonds.

Figure 12 shows the dependence of the reference surface energy on coverage.

It is clear from Figure 12 that the reference surface energy is a convex function of coverage. We can thus already state that at any fixed coverage it is more favorable for the system to split into a clean surface region in contact with a graphite-covered region. In the next section, we investigate the equilibrium of a nickel surface in contact with carbon vapor at a fixed temperature and pressure.

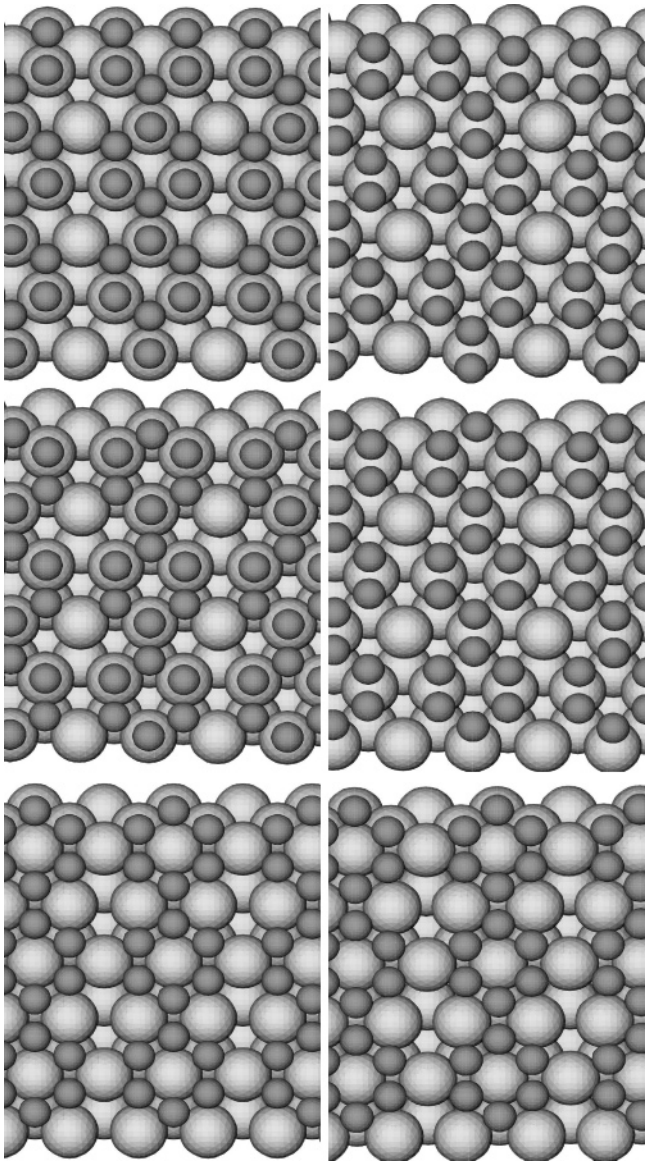

Figure 9. Carbon atoms forming rings on the nickel surface, top view. The initial configurations are on the left, and the final configurations are on the right.

5. Finite Temperature and Pressure Analysis

Using eq 14, we give a qualitative analysis of the behavior of the temperature and pressure of our system, although our simulation data are obtained for zero temperature and pressure. To start, we have calculated the surface energy of the lowest energy configurations (at 1/8, 1/4, 1/2, 3/4, and full coverages) at saturation pressure, P_{sat}, for three different temperatures, 300, 600, and 1000 K. The values of W_S to be used in eq 14, taking into account periodic boundary conditions, at various coverages are shown in Table 2.

Results are plotted in Figure 13 and summarized in Table 1.

All of the curves we obtained are clearly convex, so, based on section 2, we can conclude that the carbon on the nickel (111) surface tends to cluster, that is, the surface tends to split into the sectors covered with the graphite monolayer and empty sectors even at finite temperature. In all cases, at saturation pressure, the nickel surface is covered by graphite at equilibrium.

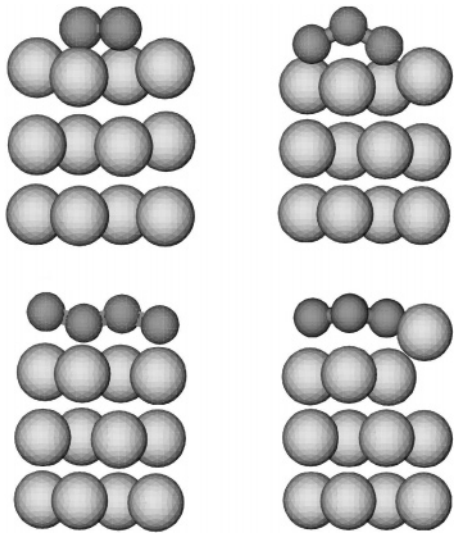

Figure 10. Side view of the lowest energy compounds: up on the left is the carbon pair, up on the right is the trimer, down on the left is the trans chain, formed by four atoms per simulation cell, and down on the right is the carbon ring, formed by six atoms per simulation cell.

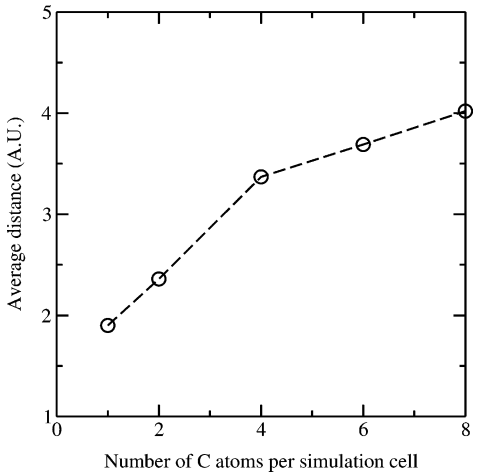

Figure 11. Average distance between carbon atoms in the lowest energy configurations and nickel surface as a function of carbon coverage. Eight atoms of carbon per simulation cell correspond to full coverage.

TABLE 1: Surface Energies as a Function of Temperature at $P = P_{sat}$ for the Lowest-Energy Configurations at Different Coverages

coverage	temperature (K)	σ (J/m^2)	coverage	temperature (K)	σ (J/m^2)
0	0	2.01	0	600	2.01
1/8	0	2.40	1/8	600	2.37
1/4	0	2.66	1/4	600	2.62
1/2	0	3.06	1/2	600	3.03
3/4	0	3.27	3/4	600	3.24
1	0	1.85	1	600	1.85
0	300	2.01	0	1000	2.01
1/8	300	2.38	1/8	1000	2.35
1/4	300	2.64	1/4	1000	2.59
1/2	300	3.04	1/2	1000	3.00
3/4	300	3.25	3/4	1000	3.22
1	300	1.85	1	1000	1.85

We have also calculated the surface energies as a function of pressure (eq 11) for all coverages at 300, 600, and 1000 K. The results are plotted in Figure 14.

At extremely low pressure, the nickel surface is clean, while at all temperatures there is a transition toward a fully covered surface at a pressure lower than the saturation pressure. This pressure is found to be closer to the saturation pressure as temperature goes up, but it also clearly appears (from the results of the previous section at 0 K) that there is no minimum temperature for the clean to fully covered transition.

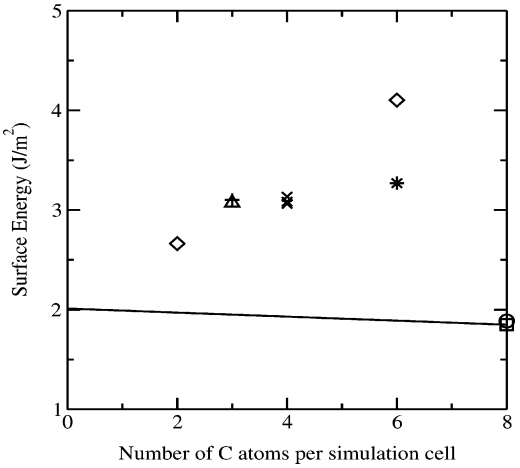

Figure 12. Surface energy as a function of the carbon coverage for carbon atoms forming compounds on the Ni(111) surface. The diamonds (◇) correspond to the compounds where half of the carbon atoms are placed in hcp and half in fcc sites, the squares (□) to the compounds where half of the carbon atoms are in on-top and half in fcc sites, and the circle (○) to the compounds where half of the carbon atoms are in on-top and half in hcp sites. The triangle (△) corresponds to the fcc−bridge−fcc, and the plus (+) corresponds to the hcp−bridge−hcp trimers. The crosses (×) correspond to the infinite trans chains. The asterisk (*) corresponds to the six atoms of carbon forming circles, all in bridge sites. The line corresponds to the surface energy described by eq 15.

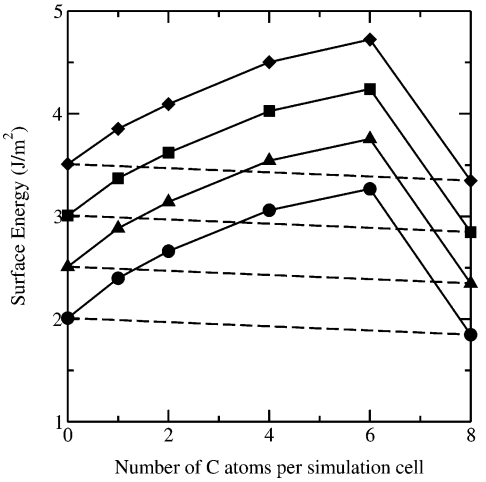

Figure 13. Surface energy as a function of the carbon coverage at 0 K (●), 300 K (▲), 600 K (■), and 1000 K (♦) for the lowest energy configurations at saturation pressure; for clarity, curves are shifted by 0.5 J/m^2 starting from the 0 K curve. Dashed lines, accidentally coincident at saturation pressure, correspond to the linear combination of the surface energies of the clean surface and complete coverage at all temperatures (eq 15).

TABLE 2

coverage	carbon compound configuration	W_s
1/8	single atom (hcp)	4
1/4	pair of atoms (hcp and fcc)	8
1/2	infinite trans chain	6
3/4	carbon rings (bridge)	4
1	graphite sheet (on-top and fcc)	1

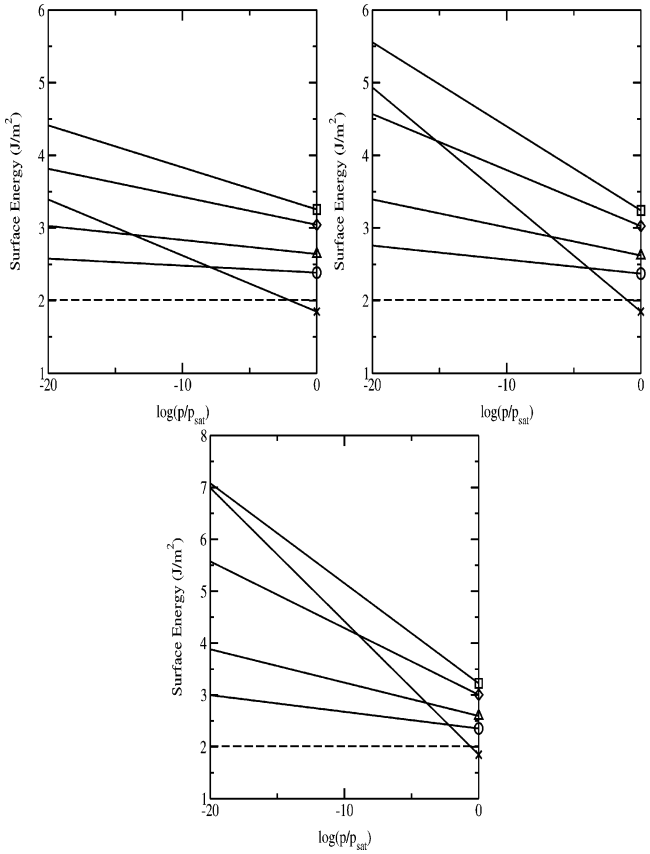

Figure 14. Surface energy as a function of pressure for the lowest energy configurations at 300 K (up left), 600 K (up right), and 1000 K (down): (○) correspond to the 1/8 coverage, (△) to 1/4 coverage, (◊) to half-coverage, (□) to 3/4 coverage, and (×) to the complete coverage. Dashed lines correspond to the surface energy of the clean nickel surface at each temperature.

6. Conclusions

The calculated carbon−nickel surface energy as a function of carbon coverage is clearly a convex function. Density functional calculations can successfully predict that stable carbon−nickel (111) surfaces are thus either clean (zero coverage) or totally covered (poisoning) by a graphitic sheet. We found that this transition occurs at carbon pressures lower than the saturation pressure at all temperatures. We also predict that, in metastable situations, carbon atoms on the nickel (111) surface will produce graphitic patches. The C−C bond is clearly essential in this mechanism, and compounds formed on the nickel surface were found to have a significantly lower energy than disperse carbon atoms. This is an important aspect of the catalytic properties of nickel surfaces.

Analysis of the lowest energy configuration for different carbon cluster sizes showed that the absorption sites for carbon atoms are different for small clusters and graphite monolayers: while on-top positions are clearly unfavorable for small carbon clusters, they become favorable in the case of a graphite monolayer. This brings two remarks: First, the mechanism of formation of the graphite monolayer from dispersed atoms must be a complex one, probably with a significant barrier (see, for example, the tortuous shape of intermediate size clusters); a study of this formation mechanism is currently in progress. Second, the placement of the atoms of the graphite monolayer indicates that the poisoning is mainly due to on-top sites.

Finally, we have found that, when the graphite monolayer is not complete, nickel atoms tend to fill the vacancies. This process of losing atoms by the nickel surface has to be compared with experimental data and with the observed diffusion of nickel inside the graphitic sheet. The interaction between nickel and carbon is a highly specific one involving a mixing of p-states of the carbon atoms and d-states of nickel.[19,20] A detailed study of this interaction at the electronic level is currently in progress.

Acknowledgment. The authors acknowledge CASPUR − Consorzio per le Appicazione del Supercalcolo per Università e Ricerca, Rome, Italy, for providing the computing resources needed to achieve this work.

References and Notes

(1) Rostrup-Nielsen, J. R. *Catalysis, Science and Technology*; Springer-Verlag: Berlin, Germany, 1983; Vol. 5.
(2) Kelley, R. D.; Goodman, D. W. *The Chemical Physics of Solid Surfaces and Heterogeneous Catalysis*; Elsevier Science Publishers: Amsterdam, The Netherlands, 1980; Vol. 4.
(3) Remediakis, I. N.; Abild-Pedersen, F.; Norskov, J. K. *J. Phys. Chem* **2004**, *108*, 14535.
(4) CPMD, Copyright IBM Corp., 1990−2001, Copyright MPI fur Festcorperforschung Stuttgart, 1997−2005.
(5) Alavi, A.; Kohanoff, J.; Parrinello, M.; Frenkel, D. *Phys. Rev. Lett.* **1994**, *73*, 2599.
(6) Feibelman, P. J.; Alavi, A. *J. Phys. Chem. B* **2004**, *108*, 14362.
(7) Al-Rawi, A. N.; Kara, A.; Rahman, T. S. *Phys. Rev. B* **2002**, *66*, 165439.
(8) Finnis, M. W.; Lozovoi, A. Y.; Alavi, A. *Annu. Rev. Matter. Res.* **2005**, *35*, 167.
(9) Kresse, G.; Hafner, J. *Surf. Sci.* **2000**, *459*, 287.
(10) Mittendorfer, F.; Hafner, J. *J. Phys. Chem.* **2002**, *106*, 13299.
(11) Troullier, N.; Martins, J. L. *Phys. Rev. B* **1991**, *43*, 1993.
(12) Perdew, J.; Burke, K.; Ernzerhof, M. *Phys. Rev. Lett.* **1996**, *77*, 3865.
(13) Hong, S.; Shin, Y.-H.; Ihm, J. *Jpn. J. Appl. Phys.* **2002**, *41*, 6142.
(14) Tyson, W. R.; Miller, W. A. *Surf. Sci.* **1977**, *62*, 267.
(15) de Boer, F. R.; Boom, R.; Mattens, W. C. M.; Miedema, A. R.; Niessen, A. K. *Cohesion in metals*; North-Holland: Amsterdam, The Netherlands, 1988.
(16) Klinke, D. J., II; Wilke, S.; Broadbelt, L. *J. Catal.* **1998**, *178*, 540.
(17) Rosei, R.; De Crescenzi, M.; Sette, F.; Quaresima, C.; Savoia, A.; Perfetti, P. *Phys. Rev. B* **1983**, *28*, 1161.
(18) Rosei, R.; Modesti, S.; Sette, F.; Quaresima, C.; Savoia, A.; Perfetti, P.; *Phys. Rev. B* **1984**, *29*, 3416.
(19) Oshima, Ch.; Nagashima, A.; *J. Phys.: Condens. Matter* **1997**, *9*, 1.
(20) Gamo, Y.; Nagashima, A.; Wakabayashi, M.; Terai, M.; Oshima, Ch. *Surf. Sci.* **1997**, *274*, 61.
(21) Souzu, Y.; Tsukada, M. *Surf. Sci.* **1995**, *326*, 42.
(22) Kawanowa, H.; Ozawa, H.; Yazaki, T.; Gotoh, Y.; Souda, R. *Jpn. J. Appl. Phys.* **2002**, *41*, 6149.
(23) Banhart, F.; Charlier, J.-C.; Ajayan P. M. *Phys. Rev. Lett.* **2000**, *84*, 686.